Geophysical Research Letters®

Author Contributions:
Conceptualization: R. A. Washenfelder, S. S. Brown, A. Franchin, A. M. Middlebrook
Data curation: R. A. Washenfelder
Formal analysis: R. A. Washenfelder, K. Ball, C. D. Holmes, R. B. Pierce
Funding acquisition: S. S. Brown
Investigation: R. A. Washenfelder, L. Azzarello, K. Ball, S. S. Brown, Z. C. J. Decker, C. D. Fredrickson, K. Hayden, C. D. Holmes, A. M. Middlebrook, B. B. Palm, R. B. Pierce, D. J. Price, J. M. Roberts, M. A. Robinson, J. A. Thornton, C. C. Womack, C. J. Young
Methodology: R. A. Washenfelder, S. S. Brown, A. Franchin, A. M. Middlebrook, M. A. Robinson

Complexity in the Evolution, Composition, and Spectroscopy of Brown Carbon in Aircraft Measurements of Wildfire Plumes

R. A. Washenfelder[1] [iD], L. Azzarello[2], K. Ball[1,3,4], S. S. Brown[1,5] [iD], Z. C. J. Decker[1,5,6] [iD], A. Franchin[1,6,7], C. D. Fredrickson[8] [iD], K. Hayden[9], C. D. Holmes[10] [iD], A. M. Middlebrook[1] [iD], B. B. Palm[7,8] [iD], R. B. Pierce[11], D. J. Price[1,6] [iD], J. M. Roberts[1] [iD], M. A. Robinson[1,5,6] [iD], J. A. Thornton[8], C. C. Womack[1,6], and C. J. Young[2] [iD]

[1]Chemical Sciences Laboratory, National Oceanic and Atmospheric Administration, Boulder, CO, USA, [2]Department of Chemistry, York University, Toronto, ON, Canada, [3]University of Maryland Baltimore County, Baltimore, MD, USA, [4]Now at: Division of Chemistry and Chemical Engineering, California Institute of Technology, Pasadena, CA, USA, [5]Department of Chemistry, University of Colorado, Boulder, CO, USA, [6]Cooperative Institute for Research in Environmental Sciences, University of Colorado, Boulder, CO, USA, [7]Now at: National Center for Atmospheric Research, Boulder, CO, USA, [8]Department of Atmospheric Sciences, University of Washington, Seattle, WA, USA, [9]Air Quality Research Division, Environment and Climate Change Canada, Toronto, ON, Canada, [10]Earth, Ocean, and Atmospheric Science, Florida State University, Tallahassee, FL, USA, [11]Space Science and Engineering Center, University of Wisconsin, Madison, WI, USA

Abstract Biomass burning is a major source of light-absorbing organic aerosol (brown carbon), but its composition, chemical evolution, and lifetime are not well known. We measured water-soluble brown carbon absorption from 310 to 500 nm on the National Oceanic and Atmospheric Administration Twin Otter aircraft during flights downwind of western United States wildfires in summer 2019. The sampling strategy was near-Lagrangian and the plume ages spanned 0–5 hr. Trends in brown carbon mass absorption coefficient with plume age varied between flights, and did not show an exponential decay over these short time scales. The measured absorption spectra were smoothly varying, without identifiable contributions from individual chromophores with structured absorption. Using aerosol tracer ions and reference absorption spectra, the calculated contribution of 4-nitrocatechol to total absorption was $<22 \pm 9\%$ and $<11 \pm 5\%$, although spectral fitting showed that it may be as low as <1.1% and <0.6% at 365 and 405 nm, respectively.

Plain Language Summary Wildfires are a major source of light-absorbing particles that affect the Earth's radiative budget, but the lifetime and composition of these particles are not well known. We measured the light absorption and concentration of water-soluble organic aerosol during aircraft flights through wildfire smoke plumes that were less than 5 hr old. We found that light absorption does not decrease over these short time scales, and may instead increase or remain constant. We examined the absorption spectra and aerosol composition to determine the contribution of individual species to the total absorption by organic aerosol.

1. Introduction

Carbonaceous aerosols may affect Earth's radiative budget by absorbing light, and are categorized as absorbing organic aerosol (brown carbon; BrC) or graphitic-like material (black carbon). Biomass burning is a major global source of both brown and black carbon (Bond et al., 2013; Laskin et al., 2015). There have been an increasing number of large fires in the western U.S. during recent decades (Burke et al., 2021), and a warmer and drier climate in the western U.S. may lead to more frequent and intense fires in the future (Barbero et al., 2015).

The chemical composition of BrC in fresh smoke and its chemical evolution downwind is not well known (Hems et al., 2021; Laskin et al., 2015). Recent studies have used liquid chromatography coupled to photodiode arrays and high-resolution mass spectrometers (e.g. Lin et al., 2016; Zhang et al., 2013) to identify absorbing organic compounds in fresh or aged biomass burning smoke from filter samples that are extracted with water, methanol, acetonitrile, or nonpolar solvents. These approaches have identified different major contributors to BrC (Fleming et al., 2020; Lin et al., 2016, 2018), possibly due to differences in combustion fuel and conditions; aerosol age and chemical processing; choice of extraction solvent; ionization methods; or the mass range of the spectrometer.

Field measurements of aged biomass burning smoke have attributed >50% of BrC absorption to nitroaromatics (Bluvshtein et al., 2017; Lin et al., 2017). Similarly, in aircraft studies downwind of western U.S. wildfires, Palm et al. (2020) found that nitroaromatics (predominantly nitrocatechol and nitrophenol) contribute 29 ± 15% of BrC absorption at 405 nm. Measurements using size-exclusion chromatography have indicated that BrC from biomass burning becomes dominated by large molecules >500 atomic mass units as it ages (Di Lorenzo & Young, 2016; Di Lorenzo et al., 2017). This is consistent with studies that find that as much as 20% of absorbing material in the near-ultraviolet (near-UV) and visible spectral range is recalcitrant against decay (Lin et al., 2016; Wong et al., 2017, 2019).

The atmospheric lifetime of BrC is not well known, largely because its composition and chemical losses have not been adequately characterized. Aging of biomass burning smoke may result in both the formation and loss of absorbing BrC chromophores. Laboratory studies of biomass burning BrC exposed to UV light and hydroxyl radical (OH) have estimated lifetimes that vary from a few hours to more than a day (Hems & Abbatt, 2018; Lin et al., 2016; Wong et al., 2017, 2019). Field studies of aged smoke from wildfires have determined BrC half-lives of 9–15 hr (Forrister et al., 2015; Wang et al., 2016), but are based on few fires. Few field measurements have reported the evolution of BrC during the first hours after emission from biomass burning.

The Fire Influence on Regional to Global Environments and Air Quality Study (FIREX-AQ) was a large, coordinated effort to sample and better understand wildfire emissions and chemistry in the western U.S. In this work, we report water-soluble BrC absorption and organic carbon concentration measured from the National Oceanic and Atmospheric Administration (NOAA) Twin Otter aircraft during downwind transects of wildfire plumes. The analysis shows that (a) the time evolution of BrC is variable and complex within the first 5 hr and is not consistent with a single exponential decay following emission; (b) Neither chemical composition nor spectral fitting are consistent with large contributions nitro-aromatic species to BrC absorption, in contrast to multiple recent analyses; and (c) Power law fits are consistent with contributions from smoothly varying chromophores or a large number of individual absorbers, indicating that the composition of the absorbing mixture is complex.

2. Experimental Approach

2.1. Overview of the FIREX-AQ Field Campaign

The FIREX-AQ field campaign included four aircraft and several mobile laboratories to examine wildfire emissions and chemistry in the western U.S. This study focuses on the "Chemistry" Twin Otter, which was based in Boise, ID and Cedar City, UT during 3 August–5 September 2019 and included instruments for gas species, aerosol species, and meteorology (Decker, Robinson, et al., 2021; Robinson et al., 2021). The Twin Otter completed 39 science flights with durations of 2.5–3 hr, and sampled nine unique wildfires in Idaho, Oregon, Nevada, Arizona, and Utah during a mixture of afternoon, evening, and night conditions. A description of instrumentation and flights is given below.

2.2. Absorption and Concentration of Water-Soluble Organic Carbon

Absorption spectra of water-soluble aerosol were measured using a particle-into-liquid sampler (PILS) coupled to a liquid waveguide capillary cell and total organic carbon analyzer (BrC-PILS), as described in Zeng et al. (2021) and the Supporting Information S1. Absorption coefficients at 310–500 nm (α) and water-soluble organic carbon (WSOC) were calculated following Hecobian et al. (2010), and are presented here as absorption in solution (Mm^{-1}) and WSOC concentration (μg C std m^{-3}). We calculate the mass absorption coefficient (MAC) as

$$\sigma_{\mathrm{MAC}}(\lambda) = \frac{\alpha(\lambda)}{[\mathrm{WSOC}]} \qquad (1)$$

in units of m^2 gC^{-1}. For absorption at 365 nm, the 3σ instrument precision was ±0.02 Mm^{-1} for 10 s flight data, and the uncertainty was ±11% (Zeng et al., 2021). For WSOC, the 3σ instrument precision was ±0.3 μgC std m^{-3} for 10 s flight data, and the calculated uncertainty was ±17%.

The BrC-PILS instrument measured water-soluble absorption, which does not include all absorbing chromophores (Liu et al., 2013). An average ratio for (methanol-soluble absorption + water-soluble absorption)/water-soluble absorption of 2.44 ± 0.03 at 365 nm and 2.26 ± 0.03 at 405 nm was determined from filter samples

of wildfire smoke acquired onboard the NASA DC-8 and analyzed following the method in Liu et al. (2014). The water-soluble absorption was multiplied by these corrections when comparing to published measurements that included methanol-soluble absorption or when considering the contribution of individual chromophores to total absorption.

2.3. Other Aircraft Measurements

The Twin Otter payload included other instruments used in this analysis, with further details provided in the SI material. Briefly, aerosol size distributions from 0.07 to 1.0 μm were measured with an optical particle counter (Brock et al., 2011). CO was measured with near-infrared cavity ring-down spectroscopy (Crosson, 2008; Karion et al., 2013). Gas-phase oxygenated organics and related species were measured with a high-resolution time-of-flight chemical-ionization mass spectrometer using iodide adduct reagent (Lee et al., 2014; Palm et al., 2019).

Aerosol composition was measured using a high-resolution time-of-flight aerosol mass spectrometer (DeCarlo et al., 2006), and used to calculate carbon oxidation state of organic aerosol (OSc; Canagaratna et al., 2015; Kroll et al., 2011). Aerosol mass spectrometer (AMS) measurements of 4-nitrocatechol were calibrated in the laboratory by comparing the sum of tracer ions at m/z 139 and 155 to total particulate nitrogen measurements (Stockwell et al., 2018).

2.4. Plume Age and Fire Radiative Power

Plume ages for each transect were calculated using back trajectory analysis (Liao et al., 2021). Fire source locations were identified based on point of ignition reported by the National Interagency Fire Center, and confirmed with MODIS and VIIRS satellite detections. Plume age was calculated as the sum of the horizontal advection age and vertical plume rise age. The horizontal advection age was calculated based on the range of ages derived from High-Resolution Rapid Refresh, North American Mesoscale Forecast System CONUS Nest, and Global Forecast System (GFS 0.25°) meteorological datasets. The vertical plume rise was assumed to be 7 m s^{-1}. The average uncertainty of the plume age for the analyzed wildfire plumes was 24% with an interquartile range of 27%.

Fire Radiative Power (FRP) was determined from Geostationary Operational Environmental Satellite (GOES-16) fire detections within ± 0.5 deg of the fire location. FRP values were calculated at the time of emission for each plume transect, based on the intercept time minus the plume age.

3. Results and Discussion

3.1. Flight Description

Table 1 summarizes a subset of the 39 science flights that were selected based on the criteria of consistent wind direction, CO enhancements greater than ~0.2 parts per million (ppm), and at least three downwind plume intercepts. Figures 1a and 1b show the selected flights, colored by water-soluble BrC and WSOC, respectively. In each flight, the Twin Otter followed the smoke plume downwind in a regular pattern of cross-wind transects, with plume ages spanning 0–5 hr. An example time series of water-soluble absorption at 365 nm, WSOC concentrations, and CO mixing ratios is shown in Figure 1c.

An examination of the evolution of BrC in downwind plumes requires that the plume sampling be approximately Lagrangian or that the fire emissions are constant. Figure 2a shows FRP at the time of emission (calculated from intercept time minus plume age) for each of the plume intercepts. FRP values for the HK163 and Granite Gulch fires are not shown, because they were below the GOES-16 detection limit. The FRP values show that each set of downwind transects sampled plumes that were emitted during slowly varying fire conditions, with the exception of two fire detections on 28 August 2019.

Figure 2b shows the difference in emission time of each plume intercept compared to the first plume intercept in the series, with a difference of 0 hr indicating that the sampled plume was emitted at the same time as the first measured plume in the series. The difference in emission time increases with plume age, because the Twin Otter intercepted downwind plumes more quickly than the smoke was advected. However, the Twin Otter's flight speed (typically 65–75 m s^{-1}) and its sampling pattern resulted in experiments that were near-Lagrangian. The

Table 1
Summary of Selected Research Flights Conducted by the NOAA Twin Otter During FIREX-AQ

Date and leg	Fire name	Fire location[a]	Num. Transects	Transect times (local time zone)	Transect plume ages[b] (h)	BrC MAC vs plume age[c] ($m^2\ gC^{-1}\ h^{-1}$)	R^2 of BrC MAC vs plume age	$\Delta Abs/\Delta CO$ vs plume age[c] ($Mm^{-1}\ ppmv^{-1}\ h^{-1}$)
9 August 2019 L2	HK 163	Oregon (45.0454, −119.4624)	10	11:47–12:54 PDT	1.1–2.9	0.31 ± 0.12	0.42	$(4.1 \pm 4.3) \times 10^{-3}$
16 August 2019 L2	Granite Gulch	Oregon (45.1781, −117.4270)	13	18:28–19:48 PDT	0.4–1.5	0.09 ± 0.08	0.10	$(1.4 \pm 1.7) \times 10^{-2}$
17 August 2019 L1	Granite Gulch	Oregon (45.1781, −117.4270)	9	17:14–18:25 PDT	0.8–1.1	1.71 ± 0.64	0.40	$(-4.1 \pm 9.5) \times 10^{-3}$
21 August 2019 L2	Castle	Arizona (36.5312, −112.2281)	8	18:04–19:04 MST	0.2–4.1	-0.14 ± 0.05	0.56	$(7.43 \pm 0.62) \times 10^{-3}$
24 August 2019 L2	204 Cow	Oregon (44.2851, −118.4598)	8	18:32–19:59 PDT	0.5–2.4	0.44 ± 0.18	0.42	$(-1.7 \pm 2.6) \times 10^{-2}$
25 August 2019 L2	204 Cow	Oregon (44.2851, −118.4598)	10	18:05–19:41 PDT	0.5–2.9	0.095 ± 0.09	0.12	$(-1.18 \pm 0.21) \times 10^{-2}$
28 August 2019 L1	204 Cow	Oregon (44.2851, −118.4598)	6	14:00–15:03 PDT	0.7–1.8	-0.035 ± 0.05	0.11	$(6.3 \pm 6.1) \times 10^{-3}$
28 August 2019 L2	204 Cow	Oregon (44.2851, −118.4598)	4	17:16–18:17 PDT	1.3–2.9	0.01 ± 0.05	0.02	$(1.22 \pm 0.33) \times 10^{-2}$
28 August 2019 L3	204 Cow	Oregon (44.2851, −118.4598)	4	20:33–21:13 PDT	2.2–4.2	-0.07 ± 0.13	0.11	$(-1.3 \pm 2.1) \times 10^{-2}$
3 September 2019 L2	204 Cow	Oregon (44.2851, −118.4598)	8	16:53–18:26 PDT	0.6–2.7	0.58 ± 0.10	0.82	$(1.00 \pm 0.49) \times 10^{-2}$
4 September 2019 L2	204 Cow	Oregon (44.2851, −118.4598)	11	17:09–18:20 PDT	0.9–2.9	0.24 ± 0.12	0.30	$(1.99 \pm 0.80) \times 10^{-2}$

[a]Point of ignition reported by the National Interagency Fire Center. [b]Plume age calculated using back trajectory reanalysis from aircraft transect to point of ignition. [c]Orthogonal distance regression fit of MAC versus plume age or Δwater-soluble BrC absorption/ΔCO versus plume age at 365 nm. The sum of methanol- and water-soluble absorption is expected to be 2.44× greater (see text).

Abbreviations: NOAA, National Oceanic and Atmospheric Administration.
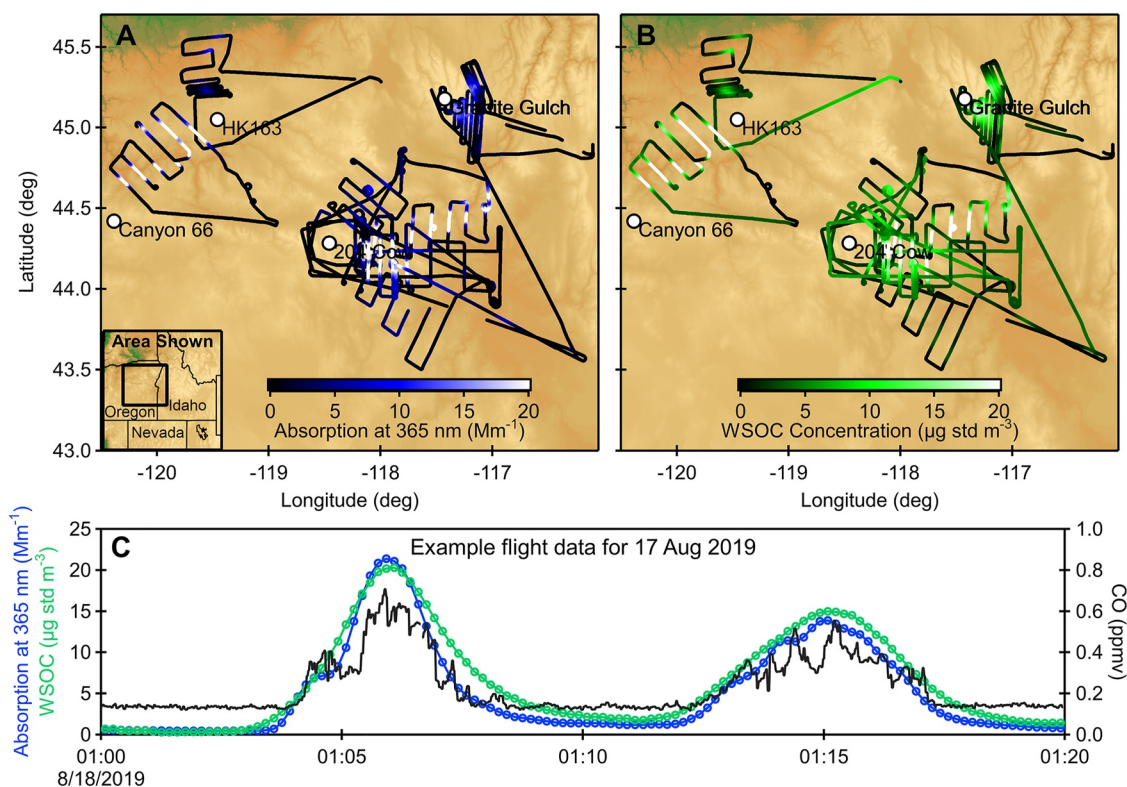
Figure 1. (a) Map of selected Twin Otter flights during FIREX-AQ, colored by water-soluble BrC absorption. 21 August 2019 flight of Castle Fire in Arizona is beyond the map area. (b) Map of selected flights, colored by WSOC concentration. (c) Time series showing water-soluble BrC absorption at 365 nm, WSOC, and CO during two plume intercepts on 17 August 2019.

consistency of the FRP and emission times of the plume transects show that it is reasonable to attribute downwind trends to chemistry and plume evolution rather than differences in initial emission conditions.

3.2. Trends in Organic Aerosol Oxidation With Plume Age

The average OSc values for each plume intercept are plotted as a function of plume age in Figure 2c. These vary between flights, but the trend within each flight shows increased oxidation, which represents oxidation of the initial plume emissions and repartitioning of volatile species between the gas and aerosol phases. The average slope for the 11 flights is 0.13 ± 0.03 hr^{-1} for the 0–5 hr plume ages measured here. Prior studies of biomass burning smoke have similarly shown that organic aerosol becomes more oxidized downwind, based on O:C ratios or the fraction of organic mass at m/z 44 (CO_2^+; an oxidation marker) (Cubison et al., 2011; Forrister et al., 2015; Garofalo et al., 2019).

3.3. Trends in BrC Absorption With Physical and Chemical Plume Age

BrC and other emitted species decrease downwind due to plume dilution. To quantify changes in absorption due to chemistry and aging, we account for dilution by normalizing the absorption measurements to WSOC or CO. Figure 2d shows BrC MAC (calculated from Equation 1) at 365 nm for the 11 selected flight legs. Linear fits (orthogonal distance regression) are shown in the figure, with slopes and uncertainties given in Table 1. The scatter in the data does not justify a more complex fit, and the variability in the magnitude and sign of the fitted slopes suggests no easily identified physical or chemical model that governs BrC evolution between fires. Although we measure water-soluble absorption continuously from 310 to 500 nm, we plot 365 nm for comparison to previous work. The trends in MAC and plume age are inconsistent between flights, and their correlation varies ($r^2 = 0.02$–0.82; median $= 0.30$). The majority of the flight legs show increasing or flat trends in MAC with
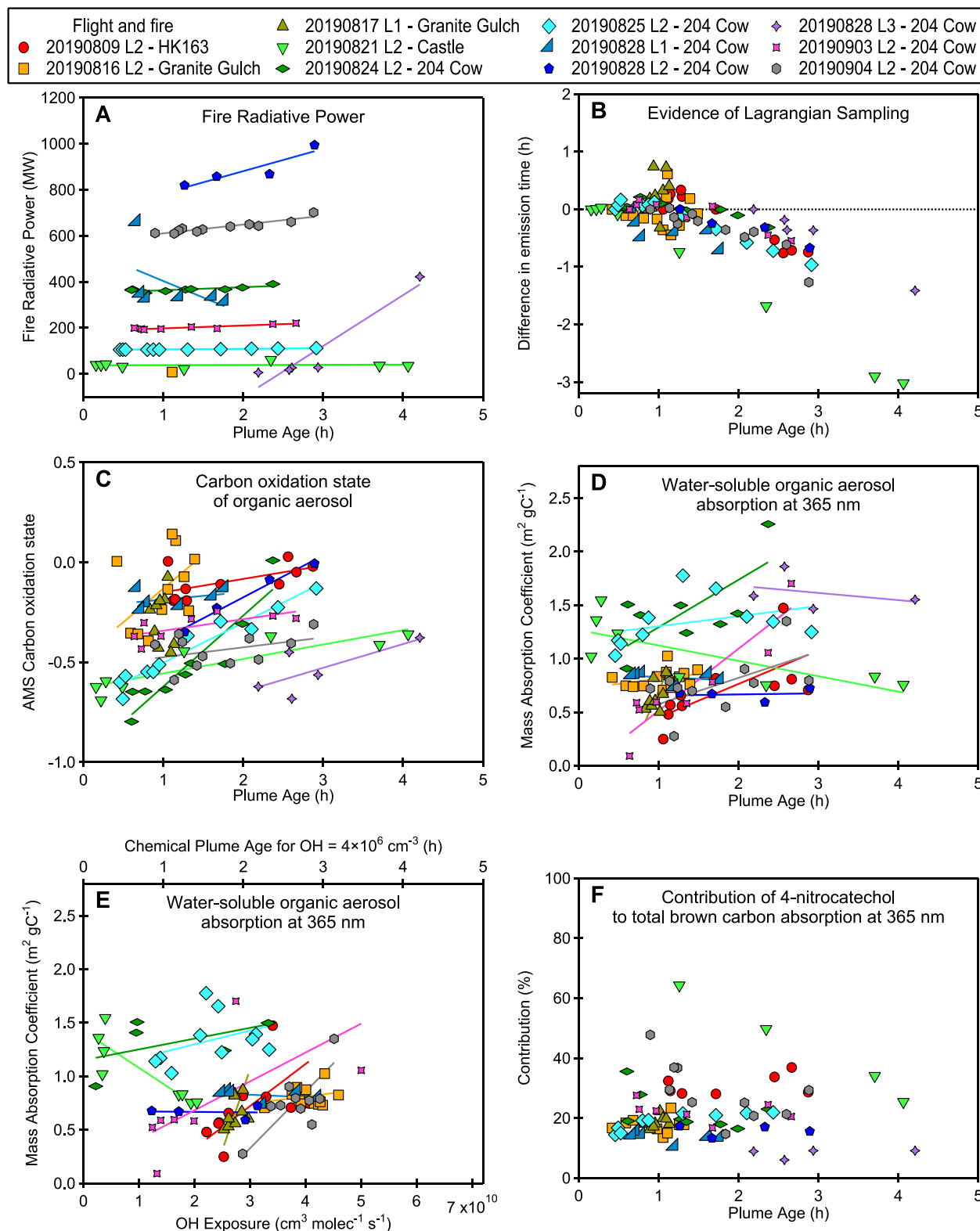
Figure 2. Each color and symbol represent a different flight leg and each point represents a single plume transect. (a) FRP for each plume transect calculated at the time of plume emission. (b) The emission time for each plume transect minus the emission time of the first plume transect in the series. (c) Carbon oxidation state for organic aerosol measured by the AMS. (d) Water-soluble BrC MAC at 365 nm as a function of plume age. (e) Water-soluble BrC MAC at 365 nm as a function of chemical plume age calculated from catechol loss for daytime transects. (f) Contribution of 4-nitrocatechol to total BrC absorption at 365 nm, calculated as an upper limit from AMS tracer ions and Hinrichs et al. (2016) absorption cross-section.

plume age, while a few show modest decreases. Potential changes in the solubility of brown carbon will affect the observed trends with plume age, and may obscure trends.

Physical plume age may not be an appropriate representation of the chemical aging of different smoke plumes, which differ in their oxidant concentrations and chemistry. Figure 2e shows BrC MAC at 365 nm plotted versus chemical plume age, calculated from measured concentrations of gas-phase catechol, CO, and their known OH reaction rates (Mellouki et al., 2021), following the method described in Roberts et al. (1984). Catechol was selected due to its rapid reaction with OH (see Supporting Information S1). Three plume intercepts from 24 August 2019 and five plume intercepts from 28 August 2019 are omitted from Figure 2e, because they occurred after sunset and would not be dominated by OH loss (Decker, Robinson, et al., 2021; Decker, Wang, et al., 2021). The majority of the flight legs show constant or increasing BrC MAC values as a function of chemical plume age, but there is no overall consistent trend.

3.4. Trends in BrC Absorption and Comparison to Prior Studies

Figure 3 shows the same 11 flights, with values of $\Delta Abs_{365nm}/\Delta CO$ for each transect. ΔCO is calculated as the average CO mixing ratio for each plume minus the average CO background outside of the plume. The average CO background is a 10 s period occurring 5 s before and after the plume intercept, with the times adjusted manually if a separate plume is intercepted during that time period. Abs_{365nm} outside of the plume was typically less than 0.2 Mm^{-1} and no background correction was made. The FIREX-AQ values in Figure 3 have been multiplied by 2.44 ± 0.03 to account for methanol-soluble absorption at 365 nm. Previously published values of $\Delta Abs_{365nm}/\Delta CO$ that included both water-soluble and methanol-soluble absorption as a function of plume age are also shown in Figure 3 (Forrister et al., 2015).

The $\Delta Abs_{365nm}/\Delta CO$ values observed during FIREX-AQ range from 0.01 to 0.28 Mm^{-1} ppbv^{-1}. For plume ages of 0–5 hr, the Forrister et al. (2015) values are similar in magnitude and within the range of the FIREX-AQ values. However, the FIREX-AQ measurements are limited to <5 hr plume ages with linear slopes varying from −0.02 to 0.02 Mm^{-1} ppbv^{-1} h^{-1} (Table 1), and do not show the steady exponential decrease in normalized BrC absorption observed by Forrister et al. (2015). If the Twin Otter had been able to track plumes further downwind, it is possible that an exponential decay observed at longer time scales (5–30 hr) would be observed. For the 0–5 hr plume ages, a similar range of O:C values is observed here (0.44–0.78) and Forrister et al. (0.45–0.75). At greater
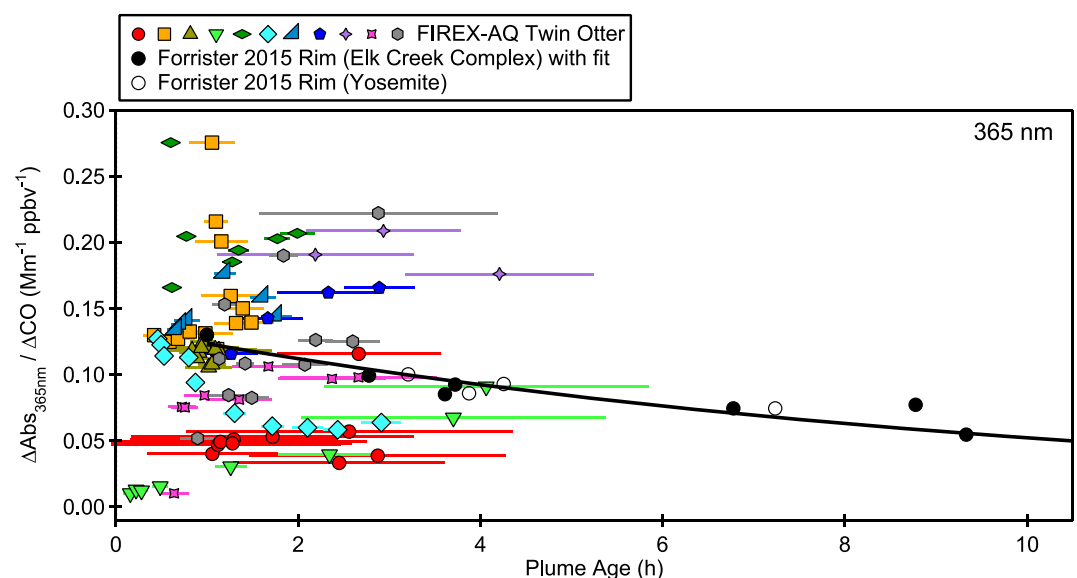
Figure 3. Normalized excess mixing ratio for BrC absorption at 365 nm/CO as a function of plume age with prior results from Forrister et al. (2015). Error bars show the uncertainty in plume age. FIREX-AQ measurements have been multiplied by 2.44 to account for absorption by methanol-soluble BrC.
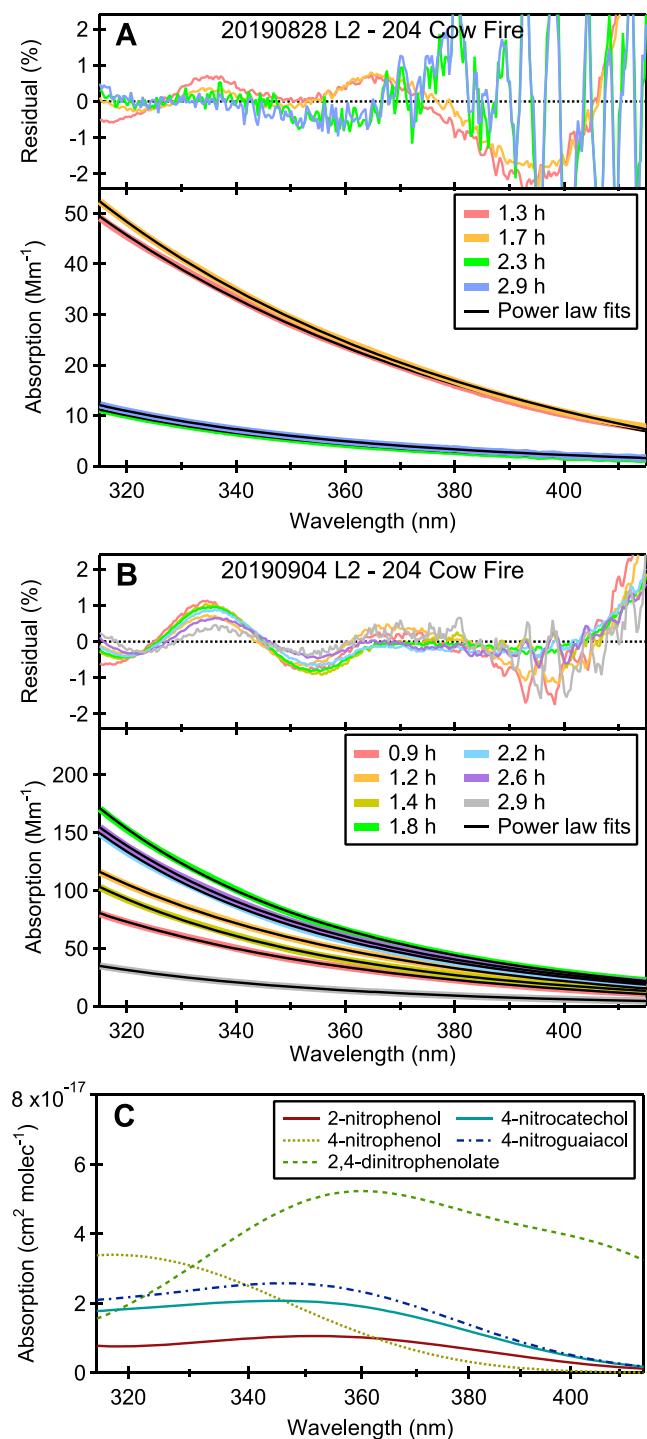
Figure 4. (a) Absorption spectra (10 s average) for downwind transects of the 204 Cow Fire on 28 August 2019 L2 for the most concentrated portion of each plume, with power law fit (black line). The upper panel shows the fit residual. (b) A similar plot showing the 204 Cow Fire on 4 September 2019 L2. (c) Absorption spectra from Hinrichs et al. (2016) for 2-nitrophenol, 4-nitrophenol, 4-nitrocatechol, 4-nitroguaiacol, and 2,4-dinitrophenolate.

plume ages, Forrister et al. shows increased O:C values of 0.8–1.0, and that greater aerosol oxidation may be linked to the decay in BrC absorption.

3.5. Constraints on Contribution by Individual Absorbing Chromophores

3.5.1. Spectral Fitting of BrC Absorption Spectra

The BrC-PILS instrument measures absorption across a broad spectral region, and provides much greater spectral information than single-wavelength methods (Lack & Langridge, 2013; Lack et al., 2012). Figures 4a and 4b show 10-s average absorption spectra in the most concentrated part of the plume transects for the 204 Cow Fire on 28 August 2019 and 4 September 2019 respectively. The absorption intensity varies downwind, as the plume is diluted. The black lines show a power law fit to each spectrum, with the form

$$\alpha(\lambda) = y_0 + k\lambda^{-AAE} \qquad (2)$$

where AAE represents the absorption Angstrom exponent (Ångström, 1929). We use the power law fit with three free parameters (y_0, k, and AAE) to examine the fitting residual for evidence of structured absorbers between 315 and 415 nm.

Nitroaromatics, particularly 4-nitrocatechol, have been previously identified as important individual contributors to BrC absorption (Bluvshtein et al., 2017; Lin et al., 2017; Mohr et al., 2013; Palm et al., 2020). Nitroaromatics are water-soluble (Achard et al., 1996; Mackay et al., 2006), and are expected to partition into aqueous solution when collected by the PILS, with absorption spectra shown in Figure 4c (Hinrichs et al., 2016) (see details in Supporting Information S1). Although these chromophores have been identified as potential contributors to BrC absorption, their absorption spectra do not demonstrate a similar shape to the residual structure from the fitted water-soluble absorption spectra.

To determine the maximum contribution of an individual absorber, we fit

$$\alpha(\lambda) = y_0 + k\lambda^{-AAE} + N\sigma(\lambda) \qquad (3)$$

where $\sigma(\lambda)$ is the literature cross-section for one absorber and N is the number density for one absorber. The fractional contribution of the absorber at a single wavelength (e.g., 365 nm) is then $N\sigma_{365nm}/\alpha_{365nm}$.

For the aqueous absorption spectra shown in Figure 4, the average absorption contributions at 365 and 405 nm are <1.9% and <1.1% for 2-nitrophenol; <1.5% and <0.1% for 4-nitrophenol; <2.6% and <1.3% for 4-nitrocatechol; <2.6% and <1.2% for 4-nitroguaiacol; and <0.1% and <0.1% for 2,4-dinitrophenolate, respectively. After correcting for the ratio of total absorption to water-soluble absorption, the summed contribution of 4-nitrocatechol to the total absorption is <1.1% at 365 nm and <0.6% at 405 nm, and the contribution of all five nitroaromatic compounds to the total absorption is <3.6% at 365 nm and <1.7% at 405 nm.

3.5.2. 4-Nitrocatechol Contribution to BrC From Mass Spectra

It is challenging to link organic aerosol mass spectra and optical properties, even when coincident, high quality field measurements are available. The majority of the organic aerosol compounds from biomass burning do not absorb light, and high resolution mass spectra are most appropriate for

examining the absorption contribution for specific target absorbers. We calculated the expected absorption by 4-nitrocatechol using its aerosol mass concentration and absorption cross-section (Hinrichs et al., 2016). The fractional contribution of 4-nitrocatechol to the total absorption at 365 nm is shown in Figure 2f. We removed plume transects with average water-soluble absorption less than 2 Mm^{-1} at 365 nm (11 out of 89 plume transects) to eliminate outliers resulting from the ratio of two small numbers. The average contribution of 4-nitrocatechol to the total absorption is $22 \pm 9\%$ at 365 nm and $11 \pm 5\%$ at 405 nm, but these values must be considered as upper limits due to the potential presence of organic ions with similar masses that cannot be resolved in the mass spectra of wildfire smoke.

A recent aircraft study of aged wildfire smoke attributed $29 \pm 15\%$ of BrC absorption at 405 nm to particulate nitrophenol and nitrocatechol isomers (Palm et al., 2020). Although our error bars overlap and there is large variability between flights, this is at least $2.6\times$ greater than the upper limit calculated here. One explanation is that our AMS mass calibration of 4-nitrocatechol using standard additions is more accurate than the values in Palm et al. (2020), which may have been affected by inlet transmission differences between the AMS and FIGAERO instruments during calibrations (see further discussion in the Supporting Information S1).

4. Conclusions

During FIREX-AQ, the NOAA Twin Otter aircraft completed 39 flights downwind of western wildfires with near-Lagrangian sampling. The in situ BrC-PILS measurements provide improved statistics about BrC evolution in aged wildfire plumes, compared to the few values reported previously. Over timescales of 0–5 hr, we observed variable trends in normalized BrC absorption. These trends contrast with the steady increases in the average carbon oxidation state of organic aerosol, and suggest that the complex evolution of BrC may be attributed to secondary photochemical reactions and gas/aerosol repartitioning. Individual absorption spectra are well-fit with a simple power law, with residuals of $\pm1\%$, indicating a complex mixture of absorbing compounds that is not dominated by individual chromophores. Future field and laboratory work is needed to better define contributions to primary and secondary BrC absorption in near-field wildfire plumes.

Data Availability Statement

The aircraft data used in the study are publicly available at https://www-air.larc.nasa.gov/missions/firex-aq/.

References

Achard, C., Jaoui, M., Schwing, M., & Rogalski, M. (1996). Aqueous solubilities of phenol derivatives by conductivity measurements. *Journal of Chemical & Engineering Data*, *41*(3), 504–507. https://doi.org/10.1021/je950202o

Ångström, A. (1929). On the atmospheric transmission of sun radiation and on dust in the air. *Geografiska Annaler*, *11*, 156–166. https://doi.org/10.2307/519399

Barbero, R., Abatzoglou, J. T., Larkin, N. K., Kolden, C. A., & Stocks, B. (2015). Climate change presents increased potential for very large fires in the contiguous United States. *International Journal of Wildland Fire*, *24*(7), 892–899. https://doi.org/10.1071/wf15083

Bluvshtein, N., Lin, P., Flores, J. M., Segev, L., Mazar, Y., Tas, E., et al. (2017). Broadband optical properties of biomass-burning aerosol and identification of brown carbon chromophores. *Journal of Geophysical Research: Atmospheres*, *122*(10), 5441–5456. https://doi.org/10.1002/2016jd026230

Bond, T. C., Doherty, S. J., Fahey, D. W., Forster, P. M., Berntsen, T., DeAngelo, B. J., et al. (2013). Bounding the role of black carbon in the climate system: A scientific assessment. *Journal of Geophysical Research: Atmospheres*, *118*(11), 5380–5552. https://doi.org/10.1002/jgrd.50171

Brock, C. A., Cozic, J., Bahreini, R., Froyd, K. D., Middlebrook, A. M., McComiskey, A., et al. (2011). Characteristics, sources, and transport of aerosols measured in spring 2008 during the aerosol, radiation, and cloud processes affecting Arctic Climate (ARCPAC) Project. *Atmospheric Chemistry and Physics*, *11*(6), 2423–2453. https://doi.org/10.5194/acp-11-2423-2011

Burke, M., Driscoll, A., Heft-Neal, S., Xue, J., Burney, J., & Wara, M. (2021). The changing risk and burden of wildfire in the United States. *Proceedings of the National Academy of Sciences*, *118*(2), 6. https://doi.org/10.1073/pnas.2011048118

Canagaratna, M. R., Jimenez, J. L., Kroll, J. H., Chen, Q., Kessler, S. H., Massoli, P., et al. (2015). Elemental ratio measurements of organic compounds using aerosol mass spectrometry: Characterization, improved calibration, and implications. *Atmospheric Chemistry and Physics*, *15*(1), 253–272. https://doi.org/10.5194/acp-15-253-2015

Crosson, E. R. (2008). A cavity ring-down analyzer for measuring atmospheric levels of methane, carbon dioxide, and water vapor. *Applied Physics B*, *92*(3), 403–408. https://doi.org/10.1007/s00340-008-3135-y

Cubison, M. J., Ortega, A. M., Hayes, P. L., Farmer, D. K., Day, D., Lechner, M. J., et al. (2011). Effects of aging on organic aerosol from open biomass burning smoke in aircraft and laboratory studies. *Atmospheric Chemistry and Physics*, *11*(23), 12049–12064. https://doi.org/10.5194/acp-11-12049-2011

DeCarlo, P. F., Kimmel, J. R., Trimborn, A., Northway, M. J., Jayne, J. T., Aiken, A. C., et al. (2006). Field-deployable, high-resolution, time-of-flight aerosol mass spectrometer. *Analytical Chemistry*, *78*(24), 8281–8289. https://doi.org/10.1021/ac061249n

Decker, Z. C. J., Robinson, M. A., Barsanti, K. C., Bourgeois, I., Coggon, M. M., DiGangi, J. P., et al. (2021). Nighttime and daytime dark oxidation chemistry in wildfire plumes: An observation and model analysis of FIREX-AQ aircraft data. *Atmospheric Chemistry and Physics Discussions*, *21*(21), 1–45. https://doi.org/10.5194/acp-21-16293-2021

Decker, Z. C. J., Wang, S., Bourgeois, I., Campuzano Jost, P., Coggon, M. M., DiGangi, J. P., et al. (2021). Novel analysis to quantify plume cross-wind heterogeneity applied to biomass burning smoke. *Environmental Science & Technology*, *55*(23), 15646–15657. https://doi.org/10.1021/acs.est.1c03803

Di Lorenzo, R. A., Washenfelder, R. A., Attwood, A. R., Guo, H., Xu, L., Ng, N. L., et al. (2017). Molecular-size-separated brown carbon absorption for biomass burning aerosol at multiple field sites. *Environmental Science & Technology*, *51*(6), 3128–3137. https://doi.org/10.1021/acs.est.6b06160

Di Lorenzo, R. A., & Young, C. J. (2016). Size separation method for absorption characterization in brown carbon: Application to an aged biomass burning sample. *Geophysical Research Letters*, *43*(1), 458–465. https://doi.org/10.1002/2015gl066954

Fleming, L. T., Lin, P., Roberts, J. M., Selimovic, V., Yokelson, R., Laskin, J., et al. (2020). Molecular composition and photochemical lifetimes of brown carbon chromophores in biomass burning organic aerosol. *Atmospheric Chemistry and Physics*, *20*(2), 1105–1129. https://doi.org/10.5194/acp-20-1105-2020

Forrister, H., Liu, J., Scheuer, E., Dibb, J., Ziemba, L., Thornhill, K. L., et al. (2015). Evolution of brown carbon in wildfire plumes. *Geophysical Research Letters*, *42*(11), 4623–4630. https://doi.org/10.1002/2015gl063897

Garofalo, L. A., Pothier, M. A., Levin, E. J. T., Campos, T., Kreidenweis, S. M., & Farmer, D. K. (2019). Emission and evolution of submicron organic aerosol in smoke from wildfires in the western United States. *ACS Earth and Space Chemistry*, *3*(7), 1237–1247. https://doi.org/10.1021/acsearthspacechem.9b00125

Hecobian, A., Zhang, X., Zheng, M., Frank, N., Edgerton, E. S., & Weber, R. J. (2010). Water-soluble organic aerosol material and the light-absorption characteristics of aqueous extracts measured over the Southeastern United States. *Atmospheric Chemistry and Physics*, *10*(13), 5965–5977. https://doi.org/10.5194/acp-10-5965-2010

Hems, R. F., & Abbatt, J. P. D. (2018). Aqueous phase photo-oxidation of brown carbon nitrophenols: Reaction kinetics, mechanism, and evolution of light absorption. *ACS Earth and Space Chemistry*, *2*(3), 225–234. https://doi.org/10.1021/acsearthspacechem.7b00123

Hems, R. F., Schnitzler, E. G., Liu-Kang, C., Cappa, C. D., & Abbatt, J. P. D. (2021). Aging of atmospheric brown carbon aerosol. *ACS Earth and Space Chemistry*, *5*(4), 722–748. https://doi.org/10.1021/acsearthspacechem.0c00346

Hinrichs, R. Z., Buczek, P., & Trivedi, J. J. (2016). Solar absorption by aerosol-bound nitrophenols compared to aqueous and gaseous nitrophenols. *Environmental Science & Technology*, *50*(11), 5661–5667. https://doi.org/10.1021/acs.est.6b00302

Karion, A., Sweeney, C., Wolter, S., Newberger, T., Chen, H., Andrews, A., et al. (2013). Long-term greenhouse gas measurements from aircraft. *Atmospheric Measurement Techniques*, *6*(3), 511–526. https://doi.org/10.5194/amt-6-511-2013

Kroll, J. H., Donahue, N. M., Jimenez, J. L., Kessler, S. H., Canagaratna, M. R., Wilson, K. R., et al. (2011). Carbon oxidation state as a metric for describing the chemistry of atmospheric organic aerosol. *Nature Chemistry*, *3*(2), 133–139. https://doi.org/10.1038/nchem.948

Lack, D. A., & Langridge, J. M. (2013). On the attribution of black and brown carbon light absorption using the Angstrom exponent. *Atmospheric Chemistry and Physics*, *13*(20), 10535–10543. https://doi.org/10.5194/acp-13-10535-2013

Lack, D. A., Langridge, J. M., Bahreini, R., Cappa, C. D., Middlebrook, A. M., & Schwarz, J. P. (2012). Brown carbon and internal mixing in biomass burning particles. *Proceedings of the National Academy of Sciences*, *109*(37), 14802–14807. https://doi.org/10.1073/pnas.1206575109

Laskin, A., Laskin, J., & Nizkorodov, S. A. (2015). Chemistry of atmospheric brown carbon. *Chemical Reviews*, *115*(10), 4335–4382. https://doi.org/10.1021/cr5006167

Lee, B. H., Lopez-Hilfiker, F. D., Mohr, C., Kurtén, T., Worsnop, D. R., & Thornton, J. A. (2014). An iodide-adduct high-resolution time-of-flight chemical-ionization mass spectrometer: Application to atmospheric inorganic and organic compounds. *Environmental Science & Technology*, *48*(11), 6309–6317. https://doi.org/10.1021/es500362a

Liao, J., Wolfe, G. M., Hannun, R. A., St Clair, J. M., Hanisco, T. F., Gilman, J. B., et al. (2021). Formaldehyde evolution in US wildfire plumes during the Fire Influence on Regional to Global Environments and Air Quality experiment (FIREX-AQ). *Atmospheric Chemistry and Physics*, *21*(24), 18319–18331. https://doi.org/10.5194/acp-21-18319-2021

Lin, P., Aiona, P. K., Li, Y., Shiraiwa, M., Laskin, J., Nizkorodov, S. A., & Laskin, A. (2016). Molecular characterization of brown carbon in biomass burning aerosol particles. *Environmental Science & Technology*, *50*(21), 11815–11824. https://doi.org/10.1021/acs.est.6b03024

Liu, J., Bergin, M., Guo, H., King, L., Kotra, N., Edgerton, E., & Weber, R. J. (2013). Size-resolved measurements of brown carbon in water and methanol extracts and estimates of their contribution to ambient fine-particle light absorption. *Atmospheric Chemistry and Physics*, *13*(24), 12389–12404. https://doi.org/10.5194/acp-13-12389-2013

Lin, P., Bluvshtein, N., Rudich, Y., Nizkorodov, S. A., Laskin, J., & Laskin, A. (2017). Molecular chemistry of atmospheric brown carbon inferred from a nationwide biomass burning event. *Environmental Science & Technology*, *51*(20), 11561–11570. https://doi.org/10.1021/acs.est.7b02276

Lin, P., Fleming, L. T., Nizkorodov, S. A., Laskin, J., & Laskin, A. (2018). Comprehensive molecular characterization of atmospheric brown carbon by high resolution mass spectrometry with electrospray and atmospheric pressure photoionization. *Analytical Chemistry*, *90*(21), 12493–12502. https://doi.org/10.1021/acs.analchem.8b02177

Liu, J. M., Scheuer, E., Dibb, J., Ziemba, L. D., Thornhill, K. L., Anderson, B. E., et al. (2014). Brown carbon in the continental troposphere. *Geophysical Research Letters*, *41*(6), 2191–2195. https://doi.org/10.1002/2013gl058976

Mackay, D., Shiu, W. Y., & Lee, S. C. (2006). *Handbook of physical-chemical properties and environmental fate for organic chemicals* (2nd ed., p. 4216). CRC Press.

Mellouki, A., Ammann, M., Cox, R. A., Crowley, J. N., Herrmann, H., Jenkin, M. E., et al. (2021). Evaluated kinetic and photochemical data for atmospheric chemistry: Volume VIII—Gas-phase reactions of organic species with four, or more, carbon atoms ($\geq C_4$). *Atmospheric Chemistry and Physics*, *21*(6), 4797–4808. https://doi.org/10.5194/acp-21-4797-2021

Mohr, C., Lopez-Hilfiker, F. D., Zotter, P., Prévôt, A. S. H., Xu, L., Ng, N. L., et al. (2013). Contribution of nitrated phenols to wood burning brown carbon light absorption in Detling, United Kingdom during winter time. *Environmental Science & Technology*, *47*(12), 6316–6324. https://doi.org/10.1021/es400683v

Palm, B. B., Liu, X., Jimenez, J. L., & Thornton, J. A. (2019). Performance of a new coaxial ion-molecule reaction region for low-pressure chemical ionization mass spectrometry with reduced instrument wall interactions. *Atmospheric Measurement Techniques*, *12*(11), 5829–5844. https://doi.org/10.5194/amt-12-5829-2019

Palm, B. B., Peng, Q., Fredrickson, C. D., Lee, B. H., Garofalo, L. A., Pothier, M. A., et al. (2020). Quantification of organic aerosol and brown carbon evolution in fresh wildfire plumes. *Proceedings of the National Academy of Sciences*, *117*(47), 29469–29477. https://doi.org/10.1073/pnas.2012218117

Roberts, J. M., Fehsenfeld, F. C., Liu, S. C., Bollinger, M. J., Hahn, C., Albritton, D. L., & Sievers, R. E. (1984). Measurements of aromatic hydrocarbon ratios and NOx concentrations in the rural troposphere: Observation of air mass photochemical aging and NOx removal. *Atmospheric Environment*, *18*(11), 2421–2432. https://doi.org/10.1016/0004-6981(84)90012-x

Robinson, M. A., Decker, Z. C. J., Barsanti, K. C., Coggon, M. M., Flocke, F. M., Franchin, A., et al. (2021). Variability and time of day dependence of ozone photochemistry in western wildfire plumes. *Environmental Science & Technology*, *55*(15), 10280–10290. https://doi.org/10.1021/acs.est.1c01963

Stockwell, C. E., Kupc, A., Witkowski, B., Talukdar, R. K., Liu, Y., Selimovic, V., et al. (2018). Characterization of a catalyst-based conversion technique to measure total particulate nitrogen and organic carbon and comparison to a particle mass measurement instrument. *Atmospheric Measurement Techniques*, *11*(5), 2749–2768. https://doi.org/10.5194/amt-11-2749-2018

Wang, X., Heald, C. L., Sedlacek, A. J., de Sá, S. S., Martin, S. T., Alexander, M. L., et al. (2016). Deriving brown carbon from multiwavelength absorption measurements: Method and application to AERONET and Aethalometer observations. *Atmospheric Chemistry and Physics*, *16*(19), 12733–12752. https://doi.org/10.5194/acp-16-12733-2016

Wong, J. P. S., Nenes, A., & Weber, R. J. (2017). Changes in light absorptivity of molecular weight separated brown carbon due to photolytic aging. *Environmental Science & Technology*, *51*(15), 8414–8421. https://doi.org/10.1021/acs.est.7b01739

Wong, J. P. S., Tsagkaraki, M., Tsiodra, I., Mihalopoulos, N., Violaki, K., Kanakidou, M., et al. (2019). Atmospheric evolution of molecular-weight-separated brown carbon from biomass burning. *Atmospheric Chemistry and Physics*, *19*(11), 7319–7334. https://doi.org/10.5194/acp-19-7319-2019

Zeng, L., Sullivan, A. P., Washenfelder, R. A., Dibb, J., Scheuer, E., Campos, T. L., et al. (2021). Assessment of online water-soluble brown carbon measuring systems for aircraft sampling. *Atmospheric Measurement Techniques*, *14*, 6357–6378. https://doi.org/10.5194/amt-14-6357-2021

Zhang, X. L., Lin, Y.-H., Surratt, J. D., & Weber, R. J. (2013). Sources, composition and absorption Angstrom exponent of light-absorbing organic components in aerosol extracts from the Los Angeles Basin. *Environmental Science & Technology*, *47*(8), 3685–3693. https://doi.org/10.1021/es305047b